J Comput Aided Mol Des (2011) 25:443–454
DOI 10.1007/s10822-011-9430-4

Rational design, synthesis and biological evaluations of amino-noscapine: a high affinity tubulin-binding noscapinoid

Pradeep K. Naik · Biswa Prasun Chatterji · Surya N. Vangapandu · Ritu Aneja · Ramesh Chandra · Srinivas Kanteveri · Harish C. Joshi

Received: 12 February 2011 / Accepted: 16 April 2011 / Published online: 5 May 2011

Abstract Noscapine and its derivatives are important microtubule-interfering agents shown to have potent anti-tumor activity. The binding free energies (ΔG_{bind}) of noscapinoids computed using linear interaction energy (LIE) method with a surface generalized Born (SGB) continuum solvation model were in agreement with the experimental ΔG_{bind} with average root mean square error of 0.082 kcal/mol. This LIE–SGB model guided us in designing a novel derivative of noscapine, amino-noscapine [(S)-3-((R)-9-amino-4-methoxy-6-methyl-5,6,7,8-tetrahydro [1, 3] dioxolo[4,5-*g*]isoquinolin-5-yl)-6,7-dimethoxy isobenzofuran-1(3*H*)-one] that has higher tubulin binding activity (predicted $\Delta G_{bind} = -6.438$ kcal/mol and experimental $\Delta G_{bind} = -6.628$ kcal/mol) than noscapine, but does not significantly change the total extent of the tubulin subunit/polymer ratio. The modes of interaction of amino-noscapine with the binding pocket of tubulin involved three hydrogen bonds and are distinct compared to noscapine which involved only one hydrogen bond. Also the patterns of non-bonded interactions are albeit different between both the lignads. The 'blind docking' approach (docking of ligand with different binding sites of a protein and their evaluations) as well as the reasonable accuracy of calculating ΔG_{bind} using LIE–SGB model constitutes the first evidence that this class of compounds binds to tubulin at a site overlapping with colchicine-binding site or close to it. Our results revealed that amino-noscapine has better anti-tumor activity than noscapine.

Keywords Noscapine · Amino-noscapine · Free energy of binding · Tubulin binding affinity · Anti-tumor activity

P. K. Naik (✉) · S. N. Vangapandu · R. Aneja · H. C. Joshi (✉)
Department of Cell Biology, Emory University School of Medicine, 615 Michael Street, Atlanta, GA 30322, USA
e-mail: pnaik2@emory.edu

H. C. Joshi
e-mail: medhcj@emory.edu

B. P. Chatterji
School of Biosciences and Bioengineering, Indian Institute of Technology, Powai, Mumbai 400076, India

R. Chandra
Dr. B. R. Ambedkar Center for Biomedical Research, University of Delhi, Delhi 110007, India

S. Kanteveri
Organic Chemistry Division-II, Indian Institute of Chemical Technology, Hyderabad 500007, India

Introduction

In our pursuit of novel orally available tubulin-binding anti-cancer agents, we discovered noscapine (1) as a structural variant of colchicine like toxin [1]. This non-narcotic opium alkaloid is used as a non-toxic anti-cough agent that binds tubulin and unlike its congener colchicine, it does not cause net depolymerization of microtubules but merely suppresses the dynamic instability of microtubules. Therefore, without changing the overall microtubule organization, it blocks mitosis at prometaphase in both healthy as well as in cancer cells. Cancer cells, however, perhaps due to the compromised checkpoints, selectively get committed to apoptosis even after removal of the drug. A favourable pharmacokinetics of this compound in vivo (clearance within ~10 h) [2, 3] and no significant side effects [4, 5] thus allows it to be therapeutic albeit at high concentrations (~150–300 mg/kg body weight) in murine models of human cancer even in cells resistant to other

anti-microtubule agents [1, 6–9]. The effectiveness of noscapine was improved by many of our efforts to decrease the dissociation constant (K_d) from 144 to 86 μM by nitro-noscapine (2), 80 μM by F-noscapine (3), 54 μM by Br-noscapine (4), 40 μM by Cl-noscapine (5), and 22 μM by I-noscapine (6) [8, 9]. This leads to develop a reasonable prediction model and guided us to rational design of more effective derivative.

Theoretical calculations, in particular the molecular docking method seems to be a proper tool for gaining such understanding. The critical issues in docking include the prediction of the correct binding pose and the accurate estimation of the corresponding binding affinity. Despite the enormous size of the conformational space for the ligands, different docking methodologies, have all been successful in reproducing the crystallographic binding modes [10–12]. However, they still need improvement when it comes to predicting binding affinities [13–15], particularly the scoring function terms responsible for the estimation of the ligand desolvation, intramolecular, and conformational entropy penalties upon binding. Since the docking algorithms provide good-quality binding poses, an energy function with a more physically reasonable description of binding contributions can be employed to rescore the docking results. This inspired us to use molecular mechanics in combination with implicit continuum solvation based scoring functions such as linear interaction energy method (LIE) with a surface generalized Born (SGB) continuum solvation model in the rescoring process [16]. The linear interaction energy approximation is a way of combining molecular mechanics calculations with experimental data to build a model scoring function for the evaluation of ligand–protein binding free energy. It has been applied on a number of protein–ligand systems with promising results producing small errors on the order of 1.0 kcal/mol for free energy prediction [16, 17]. Thus in this study we have applied this approach to design more potent noscapinoid. The predicted binding affinity has been validated by experimental evaluation.

Materials and methods

Protein preparation

The X-ray crystallographic structure of the complex between colchicine and tubulin protein (PDB ID: 1SA0, resolution 3.58 Å) [18] was used for molecular docking and rescoring. After manual inspection and cleaning of structure we retained a complex consisting of both the 'A' and 'B' chains of protein. Hydrogen were added to the model automatically via the Maestro interface (version 8.5, Schrödinger, LLC) leaving no lone pair and using an explicit all atom model. All the water molecules were removed from the complex. The multi step Schrödinger's protein preparation tool (PPrep) was used for final preparation of protein. The complex obtained was energy minimized using OPLS 2005 force field with Polak-Ribiere Conjugate Gradient (PRCG) algorithm [19]. The minimization was stopped either after 5,000 steps or after the energy gradient converged below 0.001 kcal/mol.

Ligand preparation

Molecular structures of noscapinoids (compounds 1–6) were built using molecular builder of Maestro (version 8.5). All these structures were energy minimized *in vacuo* using Impact (version 5.6, Schrödinger, LLC). Each structure was assigned an appropriate bond order using Ligprep (version 2.4, Schrödinger LLC) and optimized initially by means of the OPLS 2005 force field using default setting. Complete geometrical optimization of these structures was carried out using hybrid density functional theory with Becke's three-parameter exchange potential and the Lee–Yang–Parr correlation functional (B3LYP) [20, 21] using basis set 3-21G* level [22–24]. Jaguar (version 7.7, Schrödinger, LLC) was used for the geometrical optimization of the ligands.

Ligand docking

All ligands were docked into the tubulin receptor using Glide (version 4.5, Schrödinger, LLC) [25, 26]. After ensuring that protein and ligands are in correct form for docking, the receptor-grid file was generated using grid receptor generation program with van der Waals scaling of 0.4 Å. A grid box size of 10 Å each for the bounding and enclosing boxes were generated at the centroid of the predicted binding sites (using SiteMap, version 2.4, Schrödinger, LLC) of tubulin. The ligands were docked initially using the ''standard precision'' method and further refined using ''extra precision'' Glide algorithm. For the ligand docking stage, van der Waals scaling of the ligand was set at 0.4 Å. Out of the 50,000 poses that were sampled, 4,000 were taken through minimization (conjugate gradients 1,000) and the 30 structures that had lowest energy conformations were further evaluated for the favourable Glide docking score. A single best conformation for each ligand was considered for further rescoring.

LIE–SGB calculations

The LIE method employs experimental data on binding free energy values for a set of ligands (referred as training set) to estimate the binding affinities for a set of novel compounds. The method is based on the linear response

approximation (LRA). It demonstrates that binding free energy of a protein–ligand system is a function of polar and non-polar energy components that scale linearly with the electrostatic and van der Waals interactions between a ligand and its environment. The free energy of binding (FEB) for the complex is derived from considering only two states: (1) free ligand in the solvent and (2) ligand bound to the solvated protein. The conformational changes and entropic effects pertaining to unbound receptor are taken into account implicitly and only interactions between the ligand and either the protein or solvent are computed during molecular mechanics calculations. The SGB–LIE method also offers better accuracy in treating the long-range electrostatic interactions. The SGB–LIE method used in this study is based on the original formulation proposed by Jorgensen [16] and implemented in Liaison package (version 5.6, Schrödinger, LLC) using the OPLS-2005 force field. A novel feature of Liaison is that the simulation takes place in implicit (continuum) rather than explicit solvent, hence the name Liaison, for Linear Interaction Approximation in Implicit Solvation. The empirical relationship used by Liaison is shown below:

$$\Delta G_{\text{bind}} = \alpha\left(\langle U^{b}_{\text{vdw}}\rangle - \left\langle U^{f}_{\text{vdw}}\right\rangle\right) + \beta\left(\langle U^{b}_{\text{coul}}\rangle - \left\langle U^{f}_{\text{coul}}\right\rangle\right) + \gamma\left(\langle U^{b}_{\text{rxn}}\rangle - \langle U^{f}_{\text{rxn}}\rangle\right) + \delta\left(\langle U^{b}_{\text{cav}}\rangle - \langle U^{f}_{\text{cav}}\rangle\right) \quad (1)$$

Here $\langle\rangle$represent the ensemble average, b represents the bound form of the ligand, f represents the free form of the ligand, and α, β, γ, and δ are the coefficients. U_{vdw}, U_{coul}, U_{rxn} and U_{cav} are the van der Waals, coulombic, reaction field and cavity energy terms in the SGB continuum solvent model. The cavity energy term, U_{cav}, is proportional to the exposed surface area of the ligand. Thus, the difference: $\langle U^{b}_{\text{cav}}\rangle - \langle U^{f}_{\text{cav}}\rangle$ measures the surface area lost by contact with the receptor. The contribution for net free energy of solvation comes from two energy terms, namely reaction field energy (U_{rxn}) and cavity energy (U_{cav}): $U_{\text{SGB}} = U_{\text{rxn}} + U_{\text{cav}}$. The cavity and reaction field energy terms implicitly take into account the van der Waals and the electrostatic interactions, respectively, between the ligand and solvent. The total electrostatic energy in the SGB–LIE method is the sum of coulombic and reaction field energy terms.

The docked complex corresponding to each analog was transported to the Liaison package for subsequent LIE–SGB calculations. Sampling technique such as hybrid Monte Carlo (HMC) was used for LIE conformation space sampling. A conjugate gradient minimization was performed first, starting from the initial docked structures and then a 15 ps molecular dynamics (MD) equilibration is followed with temperature smoothly increasing from 0 to 310 K by velocity scaling and re-sampling. Finally, a 25 ps MD simulation was run for the SGB–LIE data collections. The non-bonded pair list was updated every 10 fs. The time integration step of 1.0 fs and sampling of LIE energies in every 10 steps was used. Similarly, the average LIE energies for the ligand were obtained using OPLS-2005 force field. The average LIE energy terms were used for building the binding affinity model and free energy of binding estimation for noscapine analogs. The α, β, γ, and δ LIE fitting parameters were determined using Minitab statistical package (version 15.0, Minitab Inc.) by fitting the experimental free energy of binding data on the set of molecules used.

Experimental methods

Tubulin binding assay

Microtubule proteins were isolated from mammalian brain in presence of 1 M glutamate and 10% v/v DMSO by two cycles of polymerization and depolymerization as described previously [27]. Tubulin was then purified using phosphocellulose chromatography [27, 28]. Tubulin concentration was determined by the method of Bradford [29] using bovine serum albumin (BSA) as the standard. The purified tubulin was quickly frozen as drops in liquid nitrogen and stored at −80 °C until further use.

Due to the presence of many tryptophan residues, tubulin displays an intrinsic fluorescence characteristic (excitation at 295 nm and emission at 332 nm). Like colchicine, noscapinoids change the dichroic spectrum of tubulin molecule and quench the intensity of fluorescence emission of tubulin in a concentration dependent and saturable fashion [1]. This has allowed an easy method for measuring the tubulin-noscapinoid interactions [7]. Noscapine and amino-noscapine (0–150 μM) were incubated with 2 μM tubulin in 25 mM PIPES (pH 6.8), 3 mM $MgSO_4$, and 1 mM EGTA for 30 min at 25 °C. The fluorescence intensities of tubulin in the absence and presence of different concentrations of the compounds were monitored in a JASCO FP-6500 spectrofluoremeter (JASCO, Tokyo, Japan) by exciting the samples at 295 nm and measuring the emission in the range of 310-380 nm. The inner filter effects were corrected using a formula: $F_{\text{corrected}} = F_{\text{observed}} \times \text{antilog}\,[(A_{\text{ex}} + A_{\text{em}})/2]$, where A_{ex} and A_{em} are the absorbances at the excitation and emission wavelengths. The dissociation constant (K_{d}) was estimated using the following equation: $\Delta F = \Delta F_{\text{max}}\ L/(K_{\text{d}} + L)$; where, ΔF is change in the fluorescence intensity of the tubulin upon binding to noscapine or amino-noscapine, ΔF_{max} is the maximum change in the fluorescence intensity of the protein when it is fully bound with noscapine or amino-noscapine, and L is the concentration of the ligand. ΔF was calculated by subtracting the fluorescence intensity

of tubulin in the absence of noscapine or amino-noscapine from the fluorescence intensity of tubulin in the presence of different concentrations of noscapine or amino-noscapine.

Total microtubule polymer recovery assay

Tubulin polymerization can be followed by an increase in the light scattering due to forming polymers at a given time (which are ensured to be forming microtubules by electron microscopy) and the total polymer can be examined to ensure the predominant microtubular assemblies and sedimented by ultracentrifugation. Tubulin (10 μM) was mixed with different concentrations of amino-noscapine (0, 50, 100, 150 μM) in the assembly buffer (100 mM PIPES at pH 6.8, 3 mM $MgS0_4$, 1 mM EGTA, 1 mM GTP, and 1 M sodium glutamate). A reaction control with DMSO was also set up. Polymerization was carried on by maintaining the temperature at 37 °C in the water bath for 30 min. After polymerization, the reaction mixture was centrifuged at 1,20,000×g at 30 °C for 30 min. The soluble tubulin content was measured by Bradford method [29]. Polymer mass of tubulin was found out by deducting soluble tubulin mass from the total tubulin content.

Results and discussion

Early reports have revealed that noscapinoids binds to tubulin and alters microtubule dynamics both in vitro and in vivo [1, 7]. However, where do noscapinoids bind specifically to tubulin is still not known. The best way to understand the site of interaction of ligand-receptor is to obtain the crystal structure and has not been successful so far. This is so far only possible with pure tubulin for drugs that stabilize microtubules [18, 30, 31]. Therefore we have used an approach of "blind docking" to determine the probable site of interactions of noscapinoids with tubulin which could better correlate with the experimental binding affinity. In this approach we have used the different predicted binding sites (using SiteMap, Schrödinger Inc.) of tubulin for molecular docking and evaluation of binding sites. Eventually it turns out to be the colchicine binding site of tubulin that gave better docking score for noscapinoids (Table 1)—indicating a binding site for noscapinoids overlapping with colchicine binding site [18] or a site very close to it. However, there must be some differences in the molecular interactions of noscapinoids that account for their net differences in the microtubule assembly reaction than colchicine.

The accuracy of Glide-XP docking protocol used in this study was assessed by reproducing the co-crystallized structure of colchicine in the original crystal structure of tubuline-colchicine complex (PDB ID: 1SA0, resolution 3.58 Å). This was done by moving the co-crystallized colchicine ligand outside of active site and then docking it back into the active site. The top 6 configurations after docking were taken into consideration to validate the result (Table 2). The root mean square deviation (RMSD) was calculated for each configuration in comparison to the co-crystallized colchicine and the value was found to be in between 0.19 and 1.06 Å. Whereas the RMSD value calculated out of the accepted poses for each configuration was found in between 0.35 and 0.82 Å. This revealed that the docked configurations have similar binding positions and orientations within the binding site and are similar to the crystal structure. The best docked structures, which are the configuration with the lowest Glide score, were compared with the crystal structure as shown in Fig. 1. These docking results illustrate that the best-docked colchicine complex agrees well with its crystal structure, and Glide (XP)-docking protocol successfully reproduces the crystal

Table 1 Docking results (Glide XP) of noscapine and amino-noscapine with respect to different binding sites predicted by SiteMap (Schrödinger Inc.)

Site ID	Site score	Volume	Glide XP score (kcal/mol)	
			Noscapine	Amino-noscapine
1	1.022	1483.8	−5.170	−5.766
2	1.106	220.9	−4.084	−4.749
3	0.910	236.6	−4.794	−4.971
4	0.916	127.6	−0.751	−3.869
5	0.849	138.6	−2.113	−1.742
6	0.793	170.5	−2.150	−2.385
7	0.746	67.2	−1.957	−4.263
8	0.671	84.7	−2.296	−1.336
9	0.886	85.7	−1.042	−1.302
10	0.632	80.6	−5.521	−6.461

Site 10 (correspond to colchicine binding site) is having better Glide score for both the compounds

Table 2 The RMSD and docking score from the docking simulation of 6 lowest configurations of co-crystal colchicine onto tubulin (1SA0)

Configuration	Glide score	ΔG_{score} [a]	RMSD[b] (Å)	RMSD[c] (Å)
1	−9.88	0	0.35	0.19
2	−8.94	0.94	0.45	0.24
3	−8.46	1.42	0.68	0.59
4	−8.23	1.65	0.33	0.76
5	−8.05	1.83	0.14	0.92
6	−7.64	2.24	0.82	1.06

[a] $\Delta G_{score} = E_i - E_{lowest}$

[b] RMSD, RMSD between docked poses corresponding to each configuration

[c] RMSD between docked and crystallographic colchicine structure (only heavy atoms from core rings were considered)

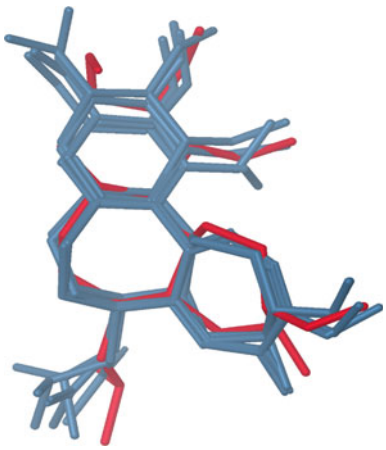

Fig. 1 Superimposition of docked configurations onto the crystal structure of colchicine (*red stick*). The RMSD (heavy atoms from core rings) = 0.19–1.06 Å

tubulin-colchicine complex. After this validation, the docking protocol was extended to both noscapine and amino-noscapine that docked at the interface of alpha and beta tubulin and well fitting the colchicine binding site (Fig. 2a–c). Consequently, the Glide docking method is a highly reliable means of reproducing the experimentally observed binding mode of noscapine and amino-noscapine to the colchicine site, since the co-crystallized structures are not yet available.

The binding mode of noscapine and amino-noscapine was visualized using MOE (Molecular Operating Environment) package (version 2008.10, Chemical Computing Group's) and was represented in two steps: (a) receptor residues that have strong interactions with the ligand, such as a favorable hydrogen-bonding interactions, and (b) receptor residues that are close to the ligand, but whose interactions with the ligand are weak or diffuse, such as hydrophobic or electrostatic interactions. The strength of hydrogen bonds (interaction score) are expressed as percentage probability from the ideal value by pairwise comparison of heavy atoms based on a scoring function that includes three parameters such as: atom types (element, hybridization, bonding environment), distance, and in-plane and out-of-plane angles of substituents [32, 33]. For example, the score with 10% would be considered a significant likelihood of being a strong hydrogen bond, whereas 1% would be considered relatively weak and 0% in the case of nonbonded residues. The mode of interactions of amino-noscapine with the residues of tubulin was distinct in comparison to noscapine (Fig. 3a, b). Three

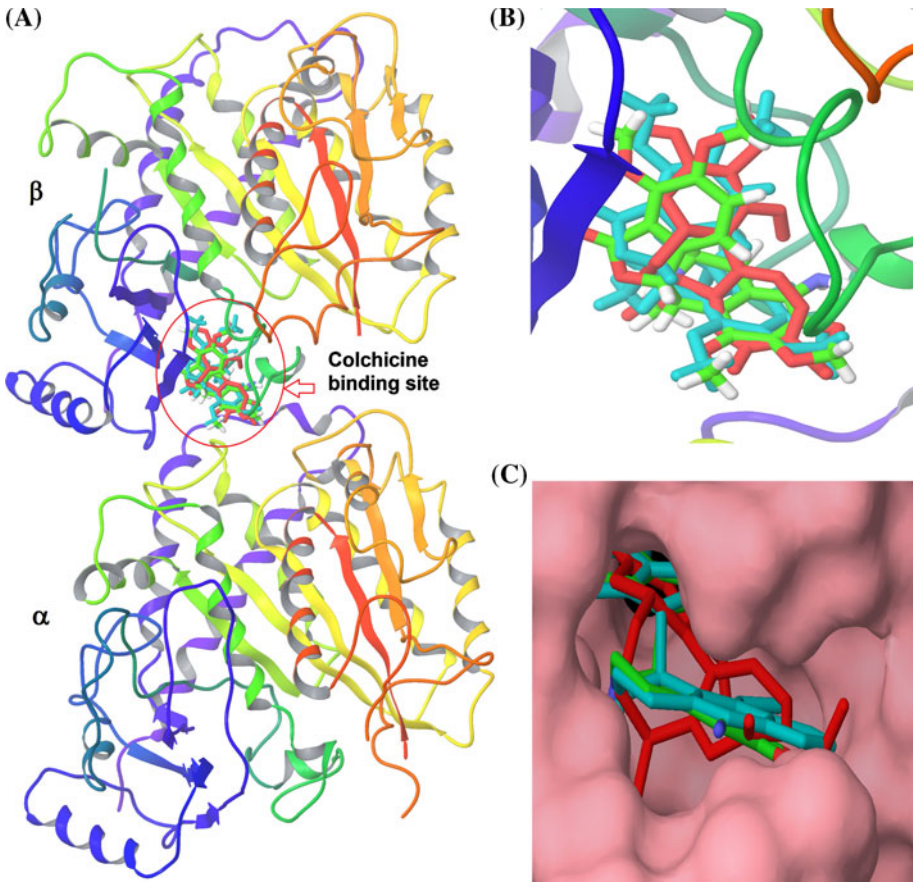

Fig. 2 Typical snapshot of **a** amino-noscapine (*green stick*) and noscapine (*blue stick*) bound to tubulin at colchicine binding site from a hybrid Monte Carlo simulation. **b** The enlarge view of the colchicine binding site with the bound ligands. **c** The bound amino-noscapine and noscapine are well-accommodated in the binding site. In the figure the co-crystalized conformation of colchicine is represented as *red sticks*

hydrogen bonds are involved in the interaction of amino-noscapine—the amino group is hydrogen bonds with the carbonyl oxygen of Val-B236 (bond length 2.0 Å, interaction score 38%) and both the oxygen atoms (O6 and O7) of dimethoxy group of isobenzofuranone ring are hydrogen bond with the side chain amide nitrogen N^{ζ} of Lys-B345 (bond length 3.0 Å, interaction score 54% and 3.5 Å, interaction score 12%) (Fig. 3a). In contrast, only one hydrogen bond between the oxygen atom (O7) of methoxy group of isobenzofuranone ring and the side chain amide nitrogen $N^{\delta 2}$ of Asn-B256 (bond length 2.9 Å, interaction score 25%) is involved in the interaction of noscapine with the binding pocket of tubulin (Fig. 3b). Further, the patterns of non-bonded interactions between amino-noscapine with the residues of tubulin are albeit different compared to noscapine (Table 3). The distinct mode of interactions (both hydrogen bonds and non-bonded interactions) with the binding pocket of tubulin revealed a better binding affinity of amino-noscapine in comparison to noscapine. Furthermore, the interaction of colchicine with the residues of tubulin involved two hydrogen bonds: the side chain atom S^{γ} of Cys-B241 hydrogen bond with the O2 and O3 atoms of colchicine (bond length 2.9 Å, interaction score 34% and 3.3 Å, interaction score 27%) (Fig. 3c). The amino acids that are uniquely involved in the interaction of colochicine are Gly-B235, Leu-B246, Asn-B247, and Thr-B362. The amino acids that are common between the noscapinoids and colchicine interactions are Val-B236, Cys-B239, Ala-B248, Lys-B252, Leu-B253, Ala-B309, Val-B311, and Ile-B364 (Fig. 3c). The overlapped docking poses of amino-noscapine (green), noscapine (blue), and colchicine (gold) at the colchicine binding site of tubulin is shown in Fig. 3d. It reveals that colchicine interactions are highly biased towards β-tubulin whereas both amino-noscapine and noscapine protrude to partially interact with α-tubulin (purple carbons) as well, indicating a binding site of noscapinoid overlapping with colchicine-binding site or close to it.

We have applied the LIE–SGB method to a data set consisting of six noscapinoids (compound number: 1–6) to build a binding affinity model applying LIE–SGB model. The energy values in Table 4 were used to fit LIE-SGB empirical equation and developed a prediction model for calculating free energy of binding (ΔG_{bind}). The calculated ΔG_{bind} represents the experimental ΔG_{bind} well. This LIE–SGB method aided the conception of amino-noscapine that had a marked drop in the free energy of binding to tubulin (−6.438 kcal/mol). This guided us to synthesize amino-noscapine derivative **(7)** and to further validate using experimental studies. The greater potency for amino-noscapine stems from better interaction with tubulin binding site as described above.

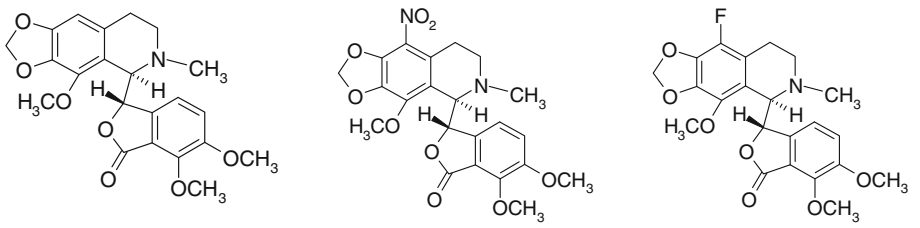

(1) **(2)** **(3)**

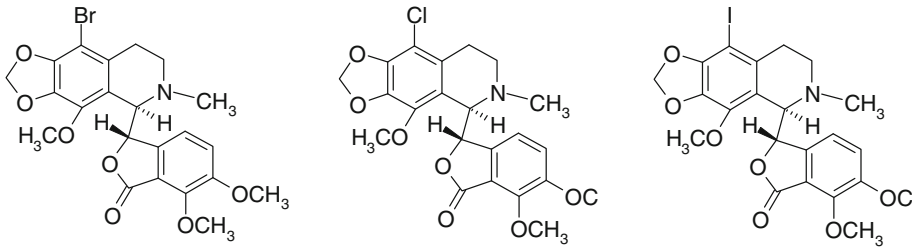

(4) **(5)** **(6)**

Synthesis of amino-noscapine

The synthetic approach of amino-noscapine from the lead compound, noscapine, is shown in Scheme 1. Briefly, noscapine was first converted into Br-noscapine by adding bromine water to a noscapine solution (in 48% hydrobromic acid) and then pH was adjusted to 10.0 with ammonia. Br-noscapine was then converted to azido-noscapine by refluxing in DMF with sodium azide and sodium iodide for 15 h. Reduction of azido derivative with tin(II) chloride in the presence of

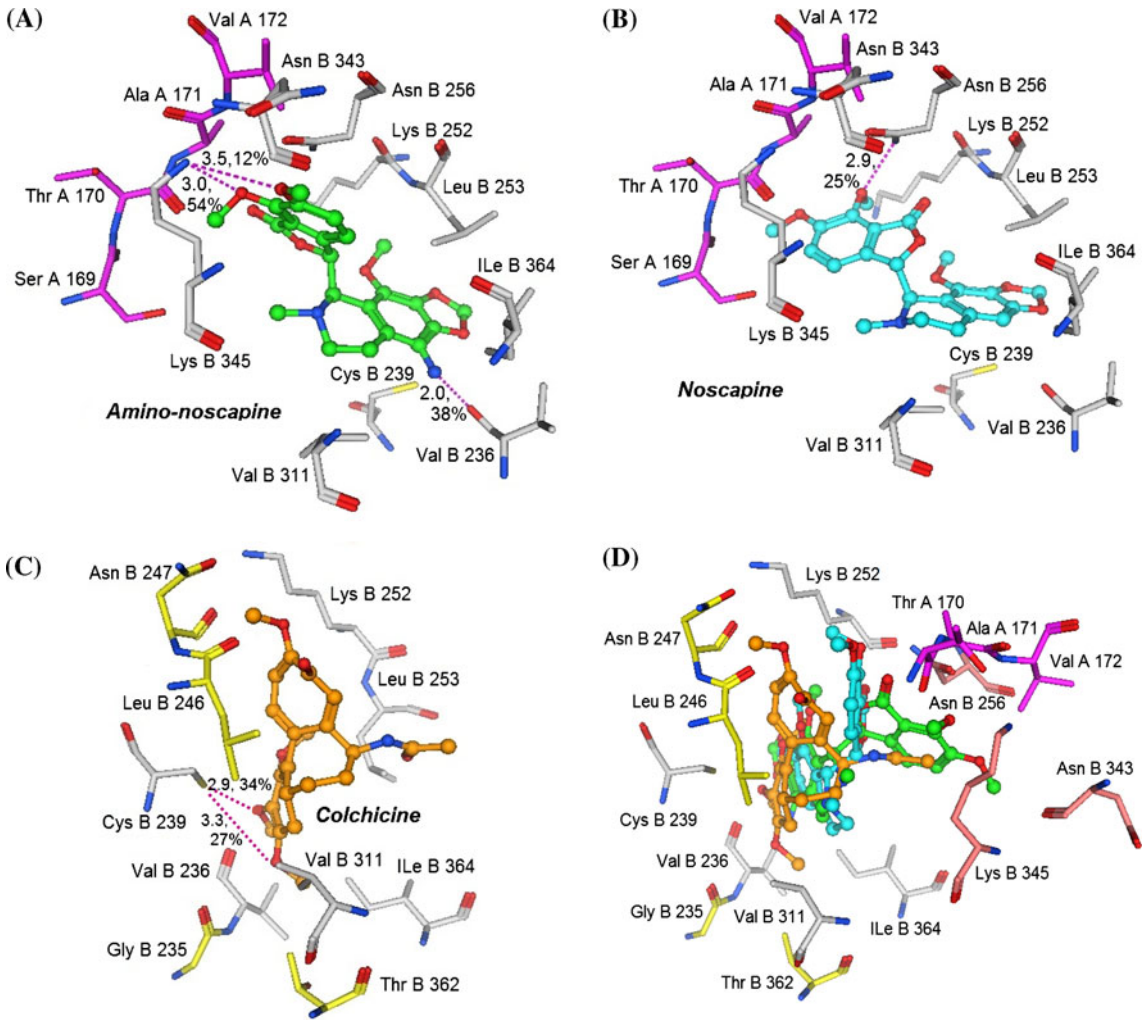

Fig. 3 Three-dimensional representation of the mode of interactions observed between: **a** tubulin and amino-noscapine, **b** tubulin and noscapine, **c** tubulin and colchicine, and **d** overlapped docking poses. The amino acids (within 4.5 Å distances from the docked ligand were only shown in the figures. **a** shows that amino-noscapine distinctly interacts with the residues of tubulin in comparison to noscapine and involved 3 hydrogen bonds (*dashed lines*): the amino group hydrogen bonds with the carbonyl oxygen of Val B 236 (bond length 2.0 Å, interaction score 38%) and both the oxygen atoms (O6 and O7) of dimethoxy groups of isobenzofuranone ring hydrogen bond with the side chain amide nitrogen (N^{ζ}) of Lys B 345 (bond length 3.0 Å, interaction score 54% and 3.5 Å, interaction score 12%). **b** shows the interaction of noscapine with the residues of tubulin that involve only one hydrogen bond (*dashed line*) between the oxygen atom (O7) of methoxy group of isobenzofuranone ring and the side chain amide nitrogen ($N^{\delta 2}$) of Asn B 256 (bond length 2.9 Å, interaction score 25%). The patterns of non-bonded interactions between amino-noscapine and noscapine with the residues of tubulin are albeit different (Table 3). **c** shows the interaction of colchicine with the residues of tubulin that involved two hydrogen bonds (*dashed lines*): the side chain atom S^{γ} of Cys B 241 establishes a hydrogen bond with the O2 and O3 atom of colchicine (bond length 2.9 Å, interaction score 34% and 3.3 Å, interaction score 27%). The amino acids that are uniquely involved in colchicine interactions have their carbon atoms colored in yellow (Gly B 235, Leu B 246, Asn B 247, Thr B 362). The other amino acids are common to the noscapinoid binding pocket. **d** shows the overlapped docking poses of amino-noscapine (*green*), noscapine (*blue*), and colchicine (*gold*) at the colchicine binding site of tubulin. Colchicine interactions are highly biased towards β-tubulin whereas both amino-noscapine and noscapine protrude to partially interact with α-tubulin (*purple carbons*) as well. Since the binding mode of colchicine is distinct and involves a set of unique amino acids in comparison to noscapine and amino-noscapine, the orientation of the binding site residues are adjusted to improve the clarity of representation of the hydrogen bonds as well as the partially overlapping of the binding poses between all three ligands in both the figures **c** and **d**. Two amino acids (Ala B 248, Ala B 309) that overlaid above the ligands have been removed to improve the clarity of representation. The geometry of hydrogen and non-bonded interactions are described in Table 3

thiophenol and triethylamine in THF for 2 h at 25 °C gave the desired compound, amino-noscapine (**7**) with 83% yield. The biological evaluation based on tubulin binding assay, total microtubule polymer recovery assay, and molecular modeling study elucidated the binding affinity, mechanism and mode of interaction of amino-noscapine to tubulin.

Table 3 Geometry of hydrogen bonds and non-bonded interactions between residues of tubulin with: (a) amino-noscapine, (b) noscapine, and (c) colchicine as represented in Fig. 3

Hydrogen bonding			*Non-bonded interaction*		
Hydrogen donor groups (HD)	Hydrogen acceptor groups (A)	Distance (Å) (H-A)	Tubulin	Ligand	Distance (Å)
(a) Interactions between tubulin and amino-noscapine					
N1'	VAL B 236 O	1.95	ILE B 364 CD1	C9'	3.62
LYS B 345 NZ	O3	2.96	LYS B 345 CE	C9	3.18
LYS B 345 NZ	O2	3.54	LYS B 345 CD	C9	3.55
			LYS B 345 CG	C9	2.93
			ASN B 343 C	C8	3.39
			VAL B 311 CG1	C8'	3.59
			VAL B 311 CB	C7'	3.82
			ALA B 309 CB	C4	3.28
			ALA B 309 CB	C5	3.50
			ALA B 309 CA	C4	3.84
			ALA B 309 CA	C5	3.63
			ASN B 256 CG	C1	3.62
			ASN B 256 CG	C7	3.68
			LEU B 253 CD2	C4'	3.83
			LEU B 253 CD2	C4	3.67
			LEU B 253 CB	C11'	3.35
			LEU B 253 CA	C11'	3.44
			LYS B 252 CB	C11'	3.34
			LYS B 252 C	C11'	3.62
			ALA B 248 CB	C11'	3.77
			ALA B 248 CB	C4'	3.75
			CYS B 239 SG	C2'	3.85
			VAL A 172 CG2	C8	3.70
			VAL A 172 CG2	C6	3.73
			ALA A 171 CA	C9	3.72
			THR A 170 C	C9	3.21
			SER A 169 C	C8	4.35

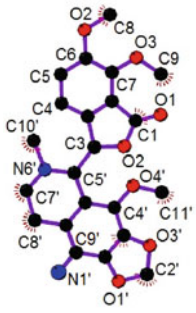

(Backbone atoms are numbered according to IUPAC) [(S)-3-((R)-9-amino-4-methoxy-6-methyl-5,6,7,8-tetrahydro [1,3] dioxolo[4,5-*g*]isoquinolin-5-yl)-6,7-dimethoxy isobenzo-furan-1(3*H*)-one]

(b) Interactions between tubulin and noscapine					
ASN B 256 ND2	O3	2.93	ILE B 364 CD1	C9'	3.10
			LYS B 345 CD	C9	3.82
			ASN B 343 C	C8	4.09
			VAL B 311 CG1	C8'	3.36
			VAL B 311 CG2	C10'	3.52
			VAL B 311 CG1	C10'	3.81
			VAL B 311 CB	C10'	3.28
			VAL B 311 CB	C8'	3.89
			ALA B 309 CB	C8'	3.62
			ALA B 309 CB	C7'	3.54
			ALA B 309 C	C8'	3.47
			ALA B 309 C	C7'	3.24
			ALA B 309 CA	C7'	3.47
			ASN B 256 CG	C1'	3.88
			LEU B 253 CD2	C4'	3.86
			LYS B 252 CE	C9	3.84
			LYS B 252 CD	C9	3.09
			LYS B 252 CG	C9	3.51
			LYS B 252 CB	C9	3.48
			ALA B 248 CA	C11'	3.12
			CYC B 239 SG	C2'	3.79
			VAL A 172 CG2	C6	4.22
			ALA A 171 CA	C9	4.38
			THR A 170 C	C8	3.06
			THR A 170 CA	C8	3.31
			SER A 169 C	C8	3.33

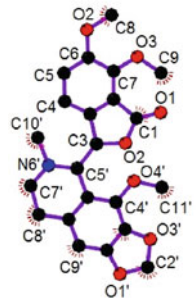

(Backbone atoms are numbered according to IUPAC) [(S)-3-((R)-4-methoxy-6-methyl-5,6,7,8-tetrahydro [1,3] dioxolo[4,5-*g*]isoquinolin-5-yl)-6,7-dimethoxy isobenzo-furan-1(3*H*)-one]

(c) Interaction between tubulin and colchicine					
CYS B 241 SG	O3	3.31	ILE B 364 CD1	C15	2.77
CYS B 241 SG	O2	2.90	ILE B 364 CG1	C15	3.77
			VAL B 311 CG1	C15	3.25
			VAL B 311 CG1	C3	3.84
			VAL B 311 CG1	C4	2.95
			VAL B 311 CB	C4	3.70
			ALA B 309 CB	C16	3.84
			LEU B 253 CD2	C13	3.65
			LEU B 253 CD2	C1	3.40
			LEU B 253 CB	C4	3.76
			LEU B 253 CA	C7	3.89
			LEU B 253 CA	C5	3.64
			LYS B 252 CB	C5	3.81
			LYS B 252 C	C5	3.71
			ALA B 248 CB	C11	3.22
			ALA B 248 CB	C12	2.87
			ALA B 248 CB	C13	3.43
			ALA B 248 CB	C1	3.881
			ALA B 248 CA	C11	2.80
			ALA B 248 CA	C12	3.19
			CYS B 239 SG	C1	3.38
			CYS B 239 SG	C2	3.09
			CYS B 239 CB	C1	3.72
			CYS B 239 CB	C2	3.83
			VAL B 236 CG1	C14	2.96
			VAL B 236 CB	C14	3.82
			VAL B 236 C	C14	3.03
			VAL B 236 CA	C15	3.40
			VAL B 236 CA	C14	3.55
			THR B 362 CG2	C15	3.43
			ASN B 247 CG	C18	2.71
			ASN B 247 CB	C18	3.27
			ASN B 247 C	C18	2.71
			ASN B 247 C	C10	3.61
			ASN B 247 C	C11	3.19
			ASN B 247 CA	C18	2.89
			LEU B 246 CD1	C7	3.20
			LEU B 246 CD1	C5	2.75
			LEU B 246 CG	C5	3.75
			LEU B 246 CB	C9	3.53
			LEU B 246 CB	C12	3.72
			LEU B 246 C	C18	2.29
			LEU B 246 C	C9	3.52
			LEU B 246 C	C10	3.26
			LEU B 246 C	C11	3.53
			LEU B 246 CA	C18	3.64
			LEU B 246 CA	C9	3.84

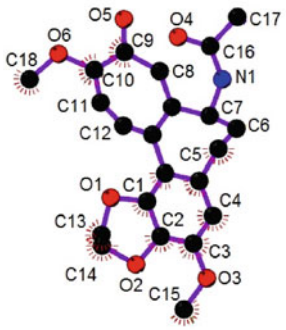

(Backbone atoms are numbered according to IUPAC) N-[(7*S*)-1,2,3,10-tetramethoxy-9-oxo-5,6,7,9-tetrahydrobenzo[*a*]heptalen-7-yl]acetamide

Table 4 Average van der Waals (vdw), coulumbic (coul), reaction field (rexn), and cavity (cav) energy terms as well as binding affinity (ΔG_{bind}) calculated based on LIE-SGB model of noscapine analogues

Ligand	$<U_{vdw}>$ (kcal/mol)	$<U_{coul}>$ (kcal/mol)	$<U_{rxn}>$ (kcal/mol)	$<U_{cav}>$ (kcal/mol)	Predicted ΔG_{bind} (kcal/mol)	Experimental ΔG_{bind} (kcal/mol)
1	−56.716	−129.510	55.227	0.679	−5.275	−5.246
2	−57.146	−49.384	56.524	1.424	−5.588	−5.551
3	−58.495	−143.070	58.490	0.637	−5.492	−5.587
4	−45.659	−113.880	59.749	1.651	−5.705	−5.827
5	−53.318	−161.240	62.265	1.536	−6.177	−6.006
6	−56.708	−173.560	50.602	2.150	−6.321	−6.360
7	−55.032	−47.025	52.602	2.930	−6.438	?

$<U_{vdw}>$, $<U_{coul}>$, $<U_{rxn}>$ and $<U_{cav}>$ energy terms represents the ensemble average energy terms calculated as the difference between bound and free state of the ligands and its environment. Experimental ΔG_{bind} was calculated from the dissociation constant (K_d value) using the relationship: $\Delta G_{bind} = RT \ln K_d$ where $T = 298$ K and $R = 0.00199$ (kcal/mol.K). Predicted ΔG_{bind} was calculated using SGB-LIE method: $\Delta G_{bind} = 0.0364\langle U_{vdw}\rangle + 0.0037\langle U_{coul}\rangle - 0.0405\langle U_{rxn}\rangle - 0.727\langle U_{cav}\rangle$. The question mark for the compound 7 indicates that the experimental binding affinity is not known but we have synthesized the compound and determined the experimental binding affinity

Scheme 1 Synthesis of amino-noscapine and its characterization

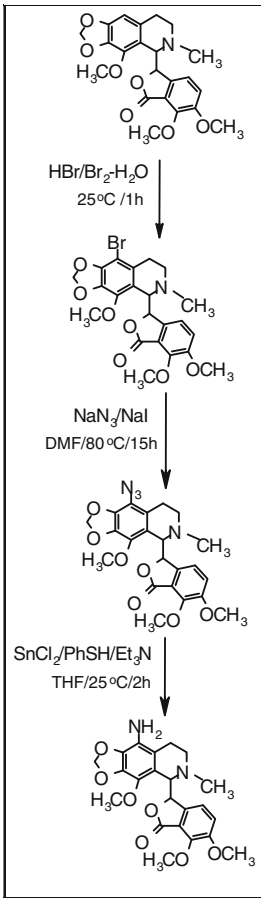

Characterization of amino-noscapine

(*S*)-3-((*R*)-9-amino-4-methoxy-6-methyl-5,6,7,8-tetrahydro-[1,3]dioxolo[4,5-*g*]isoquinolin-5-yl)-6,7-dimethoxyisobenzofuran-1(3*H*)-one : Yield, 83%; mp (HCl. Salt) 112.2-112.6 °C; IR: 1725, 1362 cm^{-1}; ^{1}H NMR ($CDCl_3$, 400 MHz): δ 7.12 (d, 1H, *J* = 7.4.0 Hz), 7.02 (d, 1H, *J* = 7.4 Hz), 6.02 (s, 2H), 5.92 (d, 1H, *J* = 4.0 Hz), 4.42 (d, 1H, *J* = 4.0 Hz), 4.20 (bs, 2H), 4.02 (s, 3H), 3.85 (s, 3H), 3.80 (s, 3H), 2.74-2.64 (m, 2H), 2.61-2.56 (m, 2H), 2.52 (s, 3H); ^{1}H NMR ($CDCl_3$ + D_2O, 400 MHz): δ 7.12 (d, 1H, *J* = 7.4.0 Hz), 7.02 (d, 1H, *J* = 7.4 Hz), 6.02 (s, 2H), 5.92 (d, 1H, *J* = 4.0 Hz), 4.42 (d, 1H, *J* = 4.0 Hz), 5.12 (bs, confirms NH_2 group), 4.02 (s, 3H), 3.85 (s, 3H), 3.80 (s, 3H), 2.74-2.64 (m, 2H), 2.61-2.56 (m, 2H), 2.52 (s, 3H); ^{13}C NMR ($CDCl_3$, 100 MHz): δ 169.5, 156.8, 152.6, 147.8, 142.7, 141.8, 135.0, 134.2, 123.2, 120.8, 119.9, 119.4, 114.1, 100.8, 87.6, 63.7, 56.8, 56.4, 56.1, 51.4, 39.2, 27.5; HRMS (ESI): *m/z* Calcd. for $C_{22}H_{24}N_2O_7$ (M+1), 428.3481; Experimentally determined, 428.1562 (M+1).

HPLC Purity and Peak Attributions:

The HPLC purity was determined following two different methods using different solvent systems.

Method 1: Ultimate Plus, LC Packings, Dionex, C_{18} column (pep Map 100, 3 μm, 100 Å particle size, ID: 1000 μm, length: 15 cm) with solvent systems A (0.1% formic acid in water) and B (acetonitrile), gradient, 25 min run at a flow of 40 μL/min. Retention time for amino-noscapine was 18.30 min. HPLC purity was 95%.

Method 2: Ultimate Plus, LC Packings, Dionex, C_{18} column (pep Map 100, 3 μm, 100 Å particle size, ID: 1000 μm, length: 15 cm) with solvent systems A (0.1% formic acid in water) and B (methanol), gradient, 25 min run at a flow of 40 μL/min. Retention time for amino-noscapine was 18.96 min. HPLC purity was 94%.

Tubulin binding activity of amino-noscapine

We found that noscapine and amino-noscapine both reduced the intrinsic fluorescence of tubulin in a concentration-dependent manner (Fig. 4a, b). The double reciprocal plots yielded a dissociation constant (K_d) of 152 ± 1 μM for noscapine binding to tubulin (Fig. 4c). Amino-noscapine was found to bind to tubulin with a K_d of 14 ± 1 μM (Fig. 4d) suggesting that amino-noscapine has a significantly higher binding affinity ($\Delta G_{bind} = -6.628$ kcal/mol) for tubulin than that of noscapine ($\Delta G_{bind} = -5.246$ kcal/mol). Experimental ΔG_{bind} was calculated from the K_d value

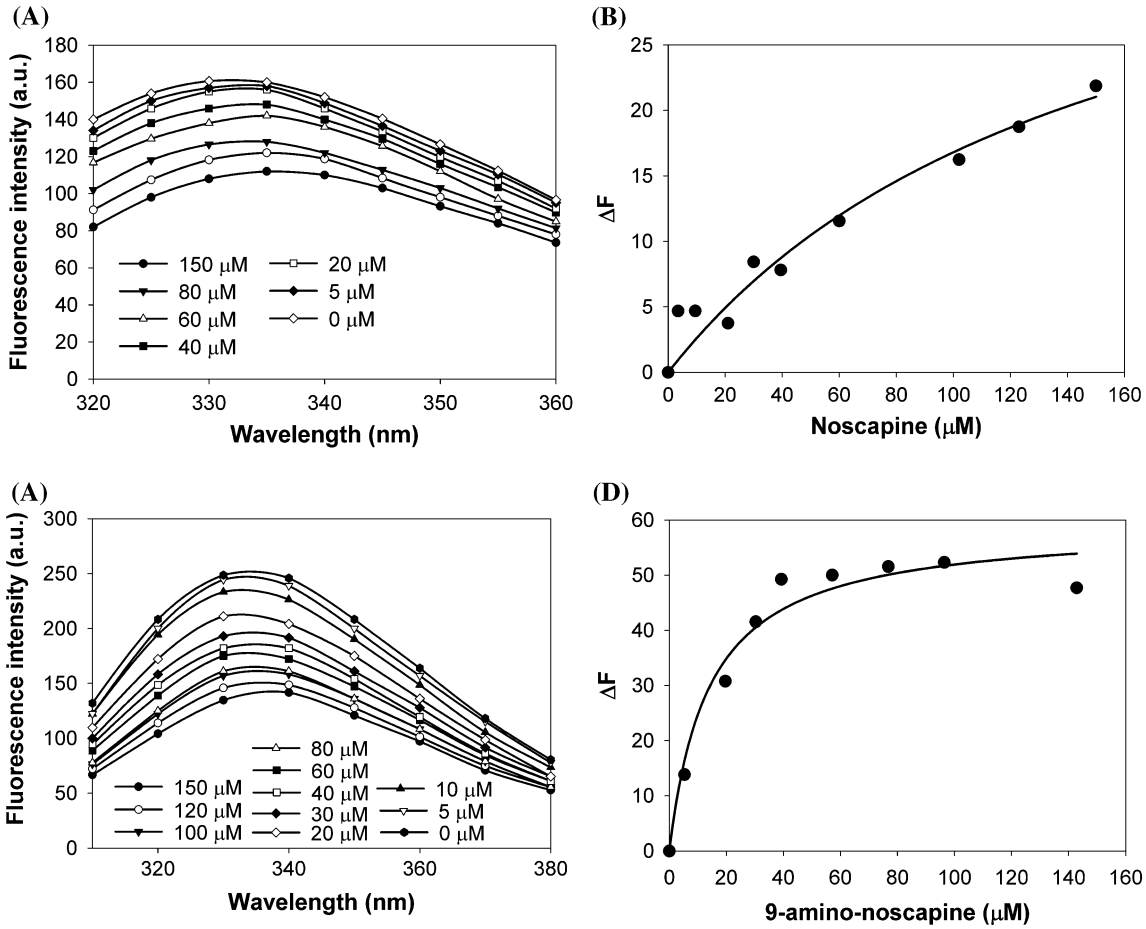

Fig. 4 The tubulin fluorescence emission intensity is quenched by noscapine (**a**) and amino-noscapine (**b**) in a concentration-dependent manner. The change in fluorescence intensity is plotted as a function of concentrations of noscapine (**c**) and amino-noscapine (**d**)

using the relationship: $\Delta G_{\text{bind}} = RT \ln K_{\text{d}}$ where $T = 298$ K and $R = 0.00199$ (kcal/mol.K). In fact, this experimentally determined value of ΔG_{bind} (−6.628 kcal/mol) turned out to be even slightly lower than the predicted value of ΔG_{bind} (−6.438 kcal/mol) for amino-noscapine suggesting that the LIE–SGB method is reasonably accurate in rational design of potent noscapinoid.

Total microtubule polymer recovery assay

We found that amino-noscapine has negligible effect on the total amount of tubulin in the form of polymeric microtubules in vitro. Even at a concentration as high as 100 μM of amino-noscapine, it did not cause microtubule depolymerization, in fact, it appeared to increase the total polymer level, albeit marginally (6.3 ± 3.8%). No evidence of abnormal twisted sheet or ring morphologies observed in colchicine induced MT-depolymerization [34] was obtained. Noscapine primarily allows the assembly of proper microtubule lattice as previously observed by electron microscopy studies [1]. Also, noscapinoids generally cause no affect on the microtubule spindle morphology of mitotically arrested cells [1, 6, 8, 9, 35–37].

Anti-tumor activity

Although the lead compound noscapine bound tubulin with a modest affinity ($K_{\text{d}} = 144$ μM) it had tested positive as an anti-cancer agent when tested against a panel of 60 human cancer cell lines by the National Cancer Institute (NCI), through its Developmental Therapeutics Program (DTP). Our rational design efforts were inspired by increasing the anti-cancer activity of the lead noscapine. Briefly, cells in the panel were treated with noscapine and amino-noscapine at increasing gradient concentrations for 48 h. The IC_{50} values that represent the drug concentrations needed to prevent cell proliferation by 50% was then measured using Sulforhodamine B assay. Figure 5 shows a bar-graph representation depicting a comparison of the IC_{50} values of both noscapine and amino-noscapine for the NCI 60 cell lines panel.

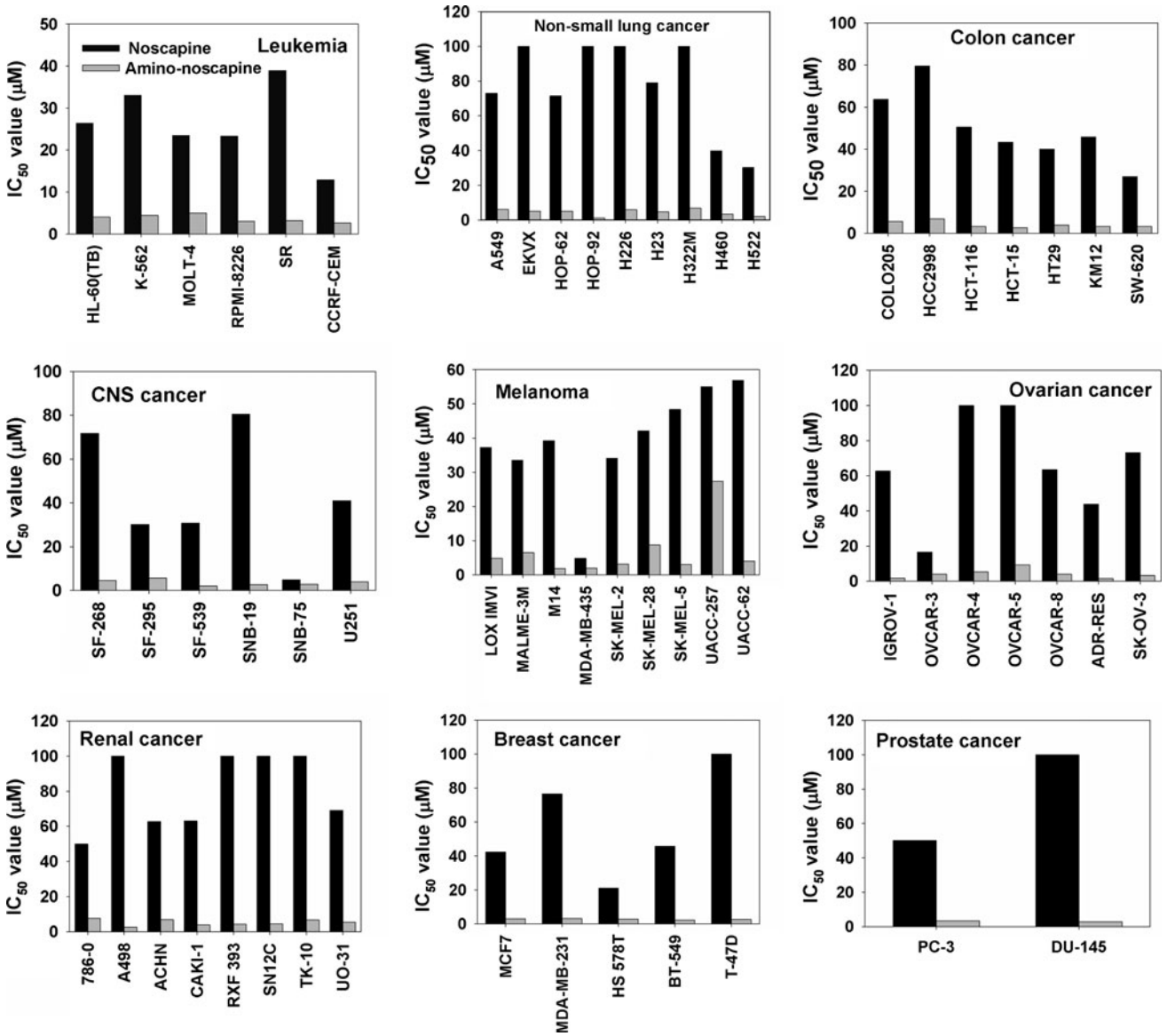

Fig. 5 Amino-noscapine is much more active than noscapine in inhibiting the proliferation of various human cancer cells. The panel of 60 human tumor cell lines is organized into subpanels representing leukemia, non-small lung cancer, colon, CNS, melanoma, renal, ovarian, breast and prostrate cancer lines. *Panels* showed *bar-graphs* depicting the comparison of IC_{50} values of noscapine (*black bars*) and amino-noscapine (*grey bars*) for cancer cell lines of various tissue origins

Conclusion

In summary, the correlation of the predicted and experimental activity turned out well with amino-noscapine as the most potent tubulin binding noscapinoid among the entire series we have published since our initial discovery of noscapine as a tubulin-binding anti-cancer agent. The present study clearly demonstrates the utility of LIE-SGB calculations for guiding this effort in the context of structure-based drug design and for providing insights into the origins of variations in activity. The current application led to the novel and most potent tubulin binding noscapinoid with increasing anti-tumor activity in comparison to the initial lead compound, noscapine. Thus, amino-noscapine indicates a great potential for further preclinical and clinical evaluation.

Acknowledgments We are thankful to Jaypee University of Information Technology, India, for providing sabbatical leave to Pradeep K. Naik. We thank Dr. Dulal panda, IIT Bombay, India, for carefully reading the manuscript and providing constructive criticisms. We are greatly indebted to the anonymous reviewers of this manuscript for extremely helpful suggestions. Grant supports: NIH grants CA-095317-01A2 (H.C. Joshi) and BOYSCAST fellowship (SR/BY/L-37/09; Department of Science and Technology, Govt. of India) to Pradeep K. Naik.

References

1. Ye K, Ke Y, Keshava N, Shanks J, Kapp IA, Tekmal RR, Petros J, Joshi HC (1998) Opium alkaloid noscapine is an antitumor agent that arrests metaphase and induces apoptosis in dividing cells. Proc Natl Acad Sci USA 95:2280–2286
2. Dahlstrom B, Mellstrand T, Lofdahl CG, Johansson M (1982) Pharmakokinetic properties of noscapine. Eur J Clin Pharmacol 22:535–539
3. Aneja R, Dhiman N, Idnani J, Awasthi A, Arora SK, Chandra R, Joshi HC (2007) Preclinical pharmacokinetics and bioavailability of noscapine, a tubulin-binding anticancer agent. Cancer Chemother Pharmacol 60(6):831–839
4. Aneja R, Kalia V, Ahmed R, Joshi HC (2007) Nonimmunosuppressive chemotherapy: EM011-treated mice mount normal T-cell responses to an acute lymphocytic choriomeningitis virus infection. Mol Cancer Ther 6(11):2891–2899
5. Aneja R, Asress S, Dhiman N, Awasthi A, Rida PC, Arora SK, Zhou J, Glass JD, Joshi HC (2010) Non-toxic melanoma therapy by a novel tubulin-binding agent. Int J Cancer 126:256–265
6. Zhou J, Panda D, Landen JW, Wilson L, Joshi HC (2002) Minor alteration of microtubule dynamics causes loss of tension across kinetochore pairs and activates the spindle checkpoint. J Biol Chem 277:17200–17208
7. Zhou J, Gupta K, Yao J, Ye K, Panda D, Giannakakou P, Joshi HC (2002) Paclitaxel-resistant human ovarian cancer cells undergo c-Jun NH2-terminal kinase-mediated apoptosis in response to noscapine. J Biol Chem 277:39777–39785
8. Aneja R, Vangapandu SN, Lopus M, Chandra R, Panda D, Joshi HC (2006) Development of a novel nitro-derivative of noscapine for the potential treatment of drug-resistant ovarian cancer and T-cell lymphoma. Mol Pharmacol 69:1801–1809
9. Aneja R, Vangapandu SN, Lopus M, Viswesarappa VG, Dhiman N, Verma A, Chandra R, Panda D, Joshi HC (2006) Synthesis of microtubule-interfering halogenated noscapine analogs that perturb mitosis in cancer cells followed by cell death. Biochem Pharmacol 72:415–426
10. Jones G, Willet P, Glen RC, Leach AR, Taylor R (1997) Development and validation of a genetic algorithm for flexible docking. J Mol Biol 267:727–748
11. Alam A, Naik PK (2009) Molecular modeling evaluation of the cytotoxic activity of podophyllotoxin analogues. J Comput Aided Mol Des 23:209–225
12. Muegge I, Martin YC (1999) A general and fast scoring function for protein-ligand interactions: a simplified potential approach. J Med Chem 42:791–804
13. Perola E, Walters WP, Charifson PS (2004) A detailed comparison of current docking and scoring methods on systems of pharmaceutical relevance. Proteins 56:235–249
14. Stahl M, Rarey M (2001) Detailed analysis of scoring functions for virtual screening. J Med Chem 44:1035–1042
15. Warren GL, Andrews CW, Capelli AM, Clarke B, LaLonde J, Lambert MH, Lindvall M, Nevins N, Semus SF, Senger S, Tedesco G, Wall ID, Woolven JM, Peishoff CE, Head MS (2006) A critical assessment of docking programs and scoring functions. J Med Chem 49:5912–5931
16. Zhou R, Frienser RA, Ghosh A, Rizzo RC, Jorgensen WL, Levy RM (2001) New linear interaction method for binding affinity calculations using a continuum solvent model. J Phys Chem B 105:10388–10397
17. Alam A, Naik PK (2009) Applying linear interaction energy method for binding affinity calculations of podophyllotoxin analogues with tubulin using continuum solvent model and prediction of cytotoxic activity. J Mol Graph Model 27: 930–943
18. Ravelli RB, Gigant B, Curmi PA, Jourdain I, Lachkar S, Sobel A, Knossow M (2004) Insight into tubulin regulation from a complex with colchicines and a stathmin-like domain. Nature 428: 198–202
19. Polak E, Ribiere G (1969) Revue Francaise Inf Rech Oper, Serie Rouge 16:35–43
20. Lee C, Yang W, Parr RG (1988) Development of the Colle-Salvetti correlation-energy formula into a functional of the electron density. Phys Rev B 37:785–789
21. Becke AD (1993) A new mixing of Hartree-Fock and local density-functional theories. J Chem Phys 98:1372–1377
22. Binkley JS, Pople JA, Hehre WJ (1980) Self-consistent molecular orbital methods. 21. Small split-valence basis sets for first-row elements. J Am Chem Soc 102:939–947
23. Gordon MS, Binkley JS, Pople JA, Pietro WJ, Hehre WJ (1982) Self-consistent molecular-orbital methods. 22. Small split-valence basis sets for second-row elements. J Am Chem Soc 104:2797–2803
24. Pietro WJ, Francl MM, Hehre WJ, Defrees DJ, Pople JA, Binkley JS (1982) Self-consistent molecular orbital methods. 24. Supplemented small split-valence basis sets for second-row elements. J Am Chem Soc 104:5039–5048
25. Friesner RA, Banks JL, Murphy RB, Halgren TA, Klicic JJ, Mainz DT, Repasky MP, Knoll EH, Shelley M, Perry JK, Shaw DE, Francis P, Shenkin PS (2004) Glide: a new approach for rapid, accurate docking and scoring. 1. Method and assessment of docking accuracy. J Med Chem 47:1739–1749
26. Halgren TA, Murphy RB, Friesner RA, Beard HS, Frye LL, Pollard WT, Banks JL (2004) Glide: a new approach for rapid, accurate docking and scoring. 2. Enrichment factors in database screening. J Med Chem 47:1750–1759
27. Hamel E, Lin CM (1981) Glutamate-induced polymerization of tubulin: characteristics of the reaction and application to the large-scale purification of tubulin. Arch Biochem Biophys 209:29–40
28. Panda D, Chakrabarti G, Hudson J, Pigg K, Miller HP, Wilson L, Himes RH (2000) Suppression of microtubule dynamic instability and treadmilling by deuterium oxide. Biochemistry 39:5075–5081
29. Bradford MM (1976) A rapid and sensitive method for the quantitation of microgram quantities of protein utilizing the principle of protein-dye binding. Anal Biochem 72:248–254
30. Nogales E, Wolf SG, Downing KH (1998) Structure of the alpha beta-tubulin dimmer by electron crystallography. Nature 391: 199–203
31. Nettles JH, Li H, Cornett B, Krahn JM, Snyderr JP, Downing KH (2004) The binding mode of epothilone A on alpha, beta-tubulin by electron crystallography. Science 305:866–869
32. Labute P (2001) Probabilistic receptor potentials. Chem Comput Group J. http://www.chemcomp.com/journal/cstat.htm
33. Clark AM, Labute P (2007) 2D depiction of protein-ligand complexes. J Chem Inf Model 47:1933–1944
34. Andreu JM, Timasheff SN (1982) Tubulin bound to colchicine forms polymers different from microtubules. Proc Natl Acad Sci USA 79:6753–6756
35. Zhou J, Gupta K, Aggarwal S, Aneja R, Chandra R, Panda D, Joshi HC (2003) Brominated derivatives of noscapine are potent microtubule-interfering agents that perturb mitosis and inhibit cell proliferation. Mol Pharmacol 63:799–807
36. Landen JW, Lang R, McMahon SJ, Rusan NM, Yvon AM, Adams AW, Sorcinelli MD, Campbell R, Bonaccorsi P, Ansel JC, Archer DR, Wadsworth P, Armstrong CA, Joshi HC (2002) Noscapine alters microtubule dynamics in living cells and inhibits the progression of melanoma. Cancer Res 62:4109–4114
37. Aneja R, Vangapandu SN, Joshi HC (2006) Synthesis and biological evaluation of a cyclic ether fluorinated noscapine analog. Bioorg Med Chem 14:8352–8358